Trajectory Sensitivity based Identification of Critical SCR for Grid-Forming and Grid-Following Converters

Bazilah Khan
Department of Electrical Engineering
Indian Institute of Technology Delhi
New Delhi, India
bazilahkhan248@gmail.com

Nilanjan Senroy
Department of Electrical Engineering
Indian Institute of Technology Delhi
New Delhi, India
nsenroy@ee.iitd.ac.in

***Abstract*—This paper presents a trajectory sensitivity-based approach for determining the critical value of the Short-Circuit Ratio (SCR) for Grid-Forming (GFM) and Grid-Following (GFL) converters, along with their comparative stability analysis. A trajectory sensitivity-based stability index, α is derived from the inverse of $\mathcal{L}_2$-norm of state sensitivity trajectories to identify the critical SCR at which instability occurs. Existing studies determine this critical value by linearly extrapolating α to zero; however, this assumption of linearity between α and the system parameter is not always valid. To address this limitation, this work proposes a revised approach based on the α curve, providing a more accurate representation of the instability boundary. The proposed approach is validated using Virtual Synchronous Generator (VSG)-based GFM and conventional GFL configurations, where results demonstrate improved accuracy in estimating the critical SCR and capture the distinct stability trends of GFM and GFL converters with respect to grid strength.**

***Index Terms*—Grid-following converter (GFL), grid-forming converter (GFM), short-circuit ratio (SCR), trajectory sensitivity, virtual synchronous generator (VSG).**

I. Introduction

Driven by the rapid increase in renewable generation, Grid-Forming (GFM) and Grid-Following (GFL) converter technologies have become indispensable to the operation and stability of modern power systems [1]–[3]. With this shift towards converter-dominated operation, system stability has become increasingly sensitive to grid strength [4], [5]. In this context, the dynamic response of GFM and GFL converters to variations in grid strength differs significantly. GFM converters, which impose their own voltage and frequency references, generally exhibit better stability under weak-grid conditions but can become unstable as the grid becomes stronger due to reduced damping and controller interaction with the stiff voltage source [6], [7]. In contrast, GFL inverters, which synchronize to the grid, tend to be stable in strong grids but may lose stability in weak grids because of the adverse interaction between the PLL and current control loops [6], [4]. This contrasting behavior highlights the importance of systematically studying inverter stability as a function of grid strength.

The Short-Circuit Ratio (SCR) is the most widely used indicator of grid strength, defined as the ratio of the rated apparent power of the grid to the short-circuit power at the point of interconnection [5]. A smaller SCR corresponds to a weaker grid and vice versa [8]. In practice, power system planners and grid codes often specify minimum SCR thresholds for stable converter operation (for instance, SCR <3 often indicates a weak grid) [9], [10]. However, these thresholds are typically derived empirically or from limited simulation studies, lacking a unified analytical basis. Consequently, determining the critical SCR, the value of SCR at which the system transitions between stability and instability, remains an open and practically important problem.

Existing techniques for assessing inverter stability under varying SCR include small-signal eigenvalue analysis, network based analysis and time-domain simulations [6], [11], [12]. While eigenvalue analysis provides valuable insights near equilibrium points, it relies on system linearization and cannot capture nonlinear or large-signal behavior. Time-domain simulations, although comprehensive, are computationally intensive and offer limited interpretability.

To overcome these limitations, Trajectory Sensitivity Analysis (TSA) provides a powerful nonlinear framework to evaluate how parameters, such as SCR, affect system trajectories over time. In contrast to eigenvalue-based small-signal sensitivity methods, TSA accounts for nonlinearities, operating point shifts, and control saturation effects. TSA measures the sensitivity of state trajectories to parameter variations, enabling the identification of critical parameter values where system responses become unbounded or unstable [13]. In earlier studies, the $\mathcal{L}_2$-norm of trajectory sensitivities has been used as a measure of system energy response, with its reciprocal, denoted as α serving as a stability index [14]. A smaller value of α indicates higher sensitivity and proximity to instability. Conventionally, α is computed for two nearby parameter values, and the critical parameter is found by linearly extrapolating α to zero [15]. However, this linear extrapolation assumes a linear dependence between α and the parameter, which is not always valid. Moreover, in some cases, the

979-8-3315-8138-1

α-curve may not intersect zero at all, making extrapolation unreliable. This paper proposes a TSA-based framework to evaluate the stability boundaries of GFL and GFM inverters with respect to SCR. Instead of relying on two data points and linear extrapolation, the proposed method computes α over a range of SCR values and identifies the minimum of the α-curve as the critical point. This approach captures the nonlinear relationship between α and SCR, providing a more realistic estimation of the instability boundary. The methodology is validated through converter-based case studies, where Virtual Synchronous Generator (VSG)-controlled GFM and PLL-based GFL configurations are analyzed.

Contributions

The main contributions of this paper are:

1) A trajectory sensitivity analysis framework to study the impact of SCR on the dynamic performance of GFL and GFM converters.
2) A novel trajectory-sensitivity-based stability index formulated as the inverse of the $\mathcal{L}_2$-norm of sensitivity trajectories for critical parameter identification.
3) An analytical method for determining critical SCR thresholds for both inverter types, eliminating reliance on empirical formulas.

II. Mathematical Background

To analyze the influence of the short-circuit ratio (SCR) on converter dynamics, a converter connected to an infinite bus through a grid impedance is considered. The grid impedance is parameterized by SCR as

$$Z_g = R_g + jX_g = \frac{V_{base}^2}{S_{base} \cdot SCR} \tag{1}$$

where V_{base} and S_{base} denote the nominal voltage and apparent power, respectively.

A. Grid-Forming (GFM) Converter Model

For Grid-Forming converter(s), a Virtual Synchronous Generator (VSG) configuration is adopted in this work. The model comprises power–frequency control (swing equation), voltage control, current control, and filter dynamics in the dq-reference frame. The detailed VSG-based GFM model is taken from [16] and can be represented in a generic nonlinear form as

$$\dot{x}_{GFM}(t) = f_{GFM}(x_{GFM}, SCR, t) \tag{2}$$

where $x_{GFM} \in \mathbb{R}^n$ is the state vector given by

$$x_{GFM} = [V_{odq}, I_{cvdq}, \gamma_{dq}, I_{odq}, \delta_{VSG}, \xi_{dq}, \omega_{VSG}] \tag{3}$$

and $t \in \mathbb{R}^+$ denotes time. The states V_{odq} and I_{odq} are the PCC voltage and grid current in the dq-frame, I_{cvdq} is the converter current, γ_{dq} and ξ_{dq} are the current and voltage controller states respectively, δ_{VSG} is the VSG angle, and ω_{VSG} is the frequency of VSG. The system is governed by a set of twelve nonlinear differential equations, with $f_{GFM} : \mathbb{R}^{n+1} \to \mathbb{R}^n$.

B. Grid-Following (GFL) Converter Model

The Grid-Following converter operates as a current-controlled voltage source synchronized to the grid via a Phase-Locked Loop (PLL). Its mathematical model, expressed in the synchronous dq-frame, comprises nonlinear differential equations governing the filter currents, dc-link voltage, and PLL dynamics. Detailed formulations and small-signal representations can be found in [17]. For TSA implementation, the GFL system is expressed in the same generic form as

$$\dot{x}_{GFL}(t) = f_{GFL}(x_{GFL}, SCR, t) \tag{4}$$

where $x_{GFL} \in \mathbb{R}^n$ is the state vector given by

$$x_{GFL} = [V_{odq}, I_{cvdq}, \gamma_{dq}, I_{odq}, \theta_{PLL}, \epsilon_{PLL}] \tag{5}$$

with $f_{GFL} : \mathbb{R}^{n+1} \to \mathbb{R}^n$ being a set of ten nonlinear differential equations. The states θ_{PLL} and ϵ_{PLL} denote the PLL phase angle and integral state, respectively.

III. Proposed Trajectory Sensitivity-Based Method

This section presents the proposed trajectory sensitivity-based framework for accurately determining the critical short-circuit ratio (SCR) of both Grid-Following (GFL) and Grid-Forming (GFM) converters. The method relies on the sensitivity of system trajectories with respect to SCR, represented by the trajectory sensitivity functions, to construct a stability index that quantifies the converter's proximity to instability. Unlike the conventional approach, which linearly extrapolates the stability index to zero, the proposed method evaluates its full nonlinear trend to determine the critical SCR more reliably.

A. Trajectory Sensitivity Formulation

For a general nonlinear dynamic system expressed in (2) and (4), the sensitivity function of the state vector $x(t)$ with respect to *SCR* as per [13] is defined as

$$s(t) = \frac{\partial x(t)}{\partial SCR}. \tag{6}$$

Taking the time derivative of (6) gives:

$$\dot{s}(t) = \frac{\partial f}{\partial x} s(t) + \frac{\partial f}{\partial SCR}, \quad s(0) = 0, \tag{7}$$

where $\frac{\partial f}{\partial x}$ represents the system Jacobian and $\frac{\partial f}{\partial \mathrm{SCR}}$ denotes the explicit parameter dependence through the grid impedance with $x \in \{x_{\mathrm{GFM}}, x_{\mathrm{GFL}}\}$ and $f \in \{f_{\mathrm{GFM}}, f_{\mathrm{GFL}}\}$.

This step transforms the algebraic sensitivity definition in (6) into a set of differential equations (7) that are integrated simultaneously with the original system (2) and (4), enabling the computation of sensitivity trajectories in the time domain. The sensitivity trajectories $s(t)$ grow rapidly when the system approaches instability, thereby providing a quantitative indicator of stability margin.

979-8-3315-8138-1

B. Trajectory Sensitivity-Based Stability Index

To measure the overall sensitivity over a finite simulation period $[0, T]$, the $\mathcal{L}_2$-norm of the trajectory sensitivities is computed as

$$\|s(t)\|_2 = \left(\int_0^T \|s(t)\|^2 \, dt \right)^{1/2}, \forall \; t > t_{\text{disturbance}} \quad (8)$$

A stability index, denoted as α, is defined as the inverse of this norm:

$$\alpha = \frac{1}{\max \|s(t)\|_2} \quad (9)$$

A larger value of α corresponds to smaller trajectory sensitivity and hence higher stability, while smaller α indicates proximity to instability. At the critical SCR, where the system transitions to instability, α approaches a minimum or tends to zero.

C. Conventional linear extrapolation method

Conventionally, the critical value of a parameter is determined by computing α at two nearby values k_1, k_2 of a parameter and linearly extrapolating it to zero [15]. This approach assumes a linear relationship between α and a parameter under consideration. For SCR, the critical value of SCR is given by:

$$\alpha(SCR^{conv}) \approx k_1 \left(SCR^{conv}\right) + k_2, \quad (10)$$

which leads to an estimated critical SCR given by the zero-crossing of the fitted line. However, practical converter systems exhibit nonlinear behavior near the stability boundary due to controller interactions, saturation effects, and grid dynamics. Consequently, the linear assumption may yield significant estimation errors or fail to detect instability if the α-curve does not intersect zero.

D. Proposed Nonlinear α-Curve method

The proposed method addresses the limitation by evaluating α over a range of SCR values

$$\Omega = [SCR_{\min}, \, SCR_{\max}] \subset \mathbb{R}^+. \quad (11)$$

to obtain its nonlinear variation to obtain α-curve, given as

$$\mathcal{A} \; = \; \alpha(\Omega) \; = \; \{\, \alpha(SCR) \in \mathbb{R}^+ \mid SCR \in \Omega \,\}. \quad (12)$$

The critical SCR is then determined as the SCR value corresponding to the minimum of this curve:

$$SCR_{crit}^{prop} = \arg\min_{\text{SCR}} \, \alpha(SCR). \quad (13)$$

The SCR corresponding to the minimum of the α-curve is treated as a candidate critical point and is subsequently verified through time-domain simulation to confirm loss of boundedness. This approach eliminates the need for extrapolation and captures the actual nonlinear trend of the stability index. The resulting α-curve provides a more physically meaningful depiction of the stability boundary, as it inherently reflects the converter–grid interactions over the entire SCR range.

IV. Results and Discussion

To validate the proposed trajectory-sensitivity-based framework, time-domain simulations were performed for both GFM and GFL converters connected to an infinite bus. The studies were carried out in MATLAB using averaged models of the converters. To excite the dynamic response, the system was subjected to a voltage dip at $t = 1$ s, reducing the voltage from 1 p.u. to 0.7 p.u. for 0.05 s. For each simulation, $x_{GFM}(t)$, $x_{GFL}(t)$, $S_{GFM}(t)$, and $S_{GFL}(t)$ were computed by numerically integrating (2), (4), and (7) using a fourth-order Runge–Kutta solver with a fixed step size of 50 μs. Subsequently, for $\Omega = [1, 20]$, the α-indices were calculated using (12). The resulting α values were plotted against *SCR* to form the α-curve for both configurations. The converter and system parameters used in the simulations are summarized in Table I, while the remaining parameters are consistent with those reported in [16] and [17].

TABLE I
Converter and System Parameters

Parameter	Value
Rated Power, S_{base}	1 MVA
Rated Voltage, V_{base}	690 V
VSG Inertia Constant, T_a	2 s
Damping Coefficient, K_d	10
PLL Controller gains, $K_{p,PLL}$, $K_{i,PLL}$	1, 10
Current Controller gains, K_{pc}, K_{ic}	0.1, 10
Voltage Controller gains, K_{pv}, K_{iv}	10, 10

A. Grid-Forming Converter (GFM) Results

Figures 1– 4 present the results for the VSG-based GFM converter. The α-curve in Fig. 1 demonstrates a distinctly nonlinear dependence on SCR. The GFM converter exhibited a tendency to lose stability as the grid became stiffer, which is in accordance with an inherent characteristic arising from reduced virtual damping and control interaction with a grid voltage source [6]. On the other hand, it remained stable under weak-grid conditions. The conventional linear extrapolation method predicted a critical value of $SCR_{crit}^{conv} = 9.47$. However, the proposed nonlinear approach identified the true critical SCR as $SCR_{crit}^{prop} = 11.95$, corresponding to the minimum of the α-curve. This discrepancy confirmed that α did not vary linearly with SCR near the instability boundary. To verify the predicted critical SCR, time-domain simulations were performed at different SCR values and at the critical values of SCR estimated using conventional SCR_{crit}^{conv} and proposed SCR_{crit}^{prop} methods. The transient responses of the virtual rotor angle δ_{VSG} and frequency deviation $\Delta\omega_{VSG}$, shown in Figs. 2 and 3 indicate that for $SCR < 11.95$, the system remained stable with well-damped oscillations. At $SCR = 11.95$, oscillations in δ_{VSG} and $\Delta\omega_{VSG}$ diverged, indicating the onset of instability and confirming the predicted critical SCR.

The phase portrait in Fig. 4 further supports this observation. Trajectories corresponding to the stable case did not converge to the equilibrium point but exhibit outward spiraling motion.

979-8-3315-8138-1

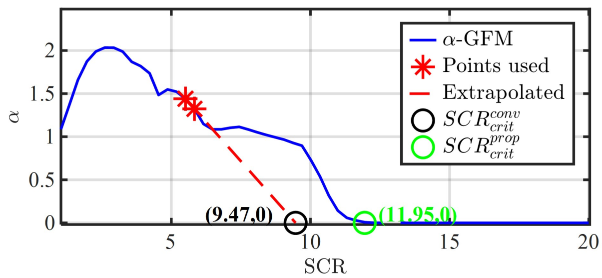

Fig. 1. Variation of the trajectory-sensitivity-based stability index α with SCR for VSG (GFM).

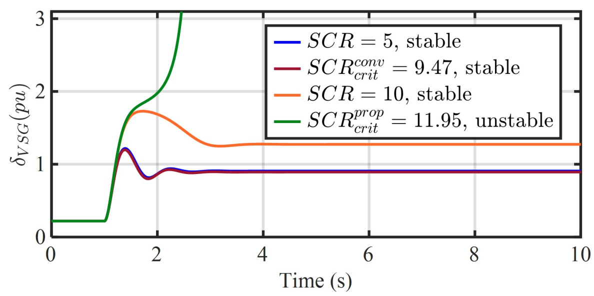

Fig. 2. Virtual rotor angle response of VSG under varying grid strengths.

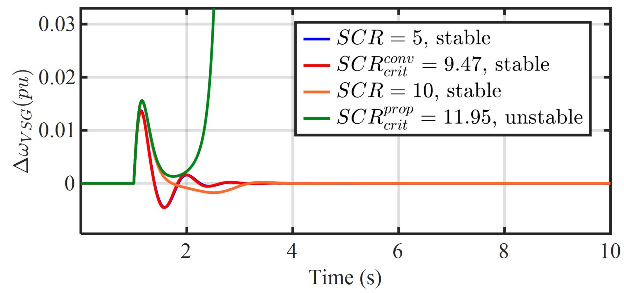

Fig. 3. Frequency deviation of VSG under varying grid strengths.

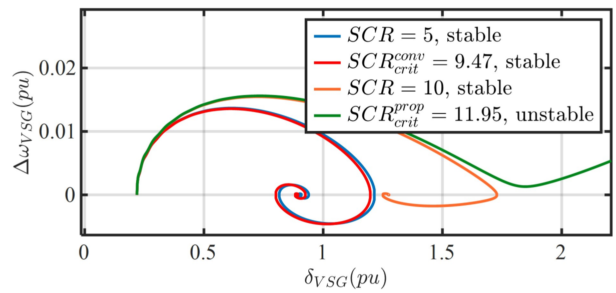

Fig. 4. Phase portraits illustrating stability transition in VSG (GFM).

This shift represents a change in the initial value of the virtual rotor angle, leading to a new steady state in the stable case, while, in the unstable condition, the trajectories diverged.

B. Grid-Following Converter (GFL) Results

The corresponding results for the GFL converter are depicted in Figs. 5– 8. Similar to the GFM case, the α-curve in Fig. 5 exhibits strong nonlinearity. In contrast to GFM behavior, GFL converters maintained stability under strong-grid conditions but lost synchronism in weak grids due to adverse coupling between the PLL and current-control loops. The conventional linear extrapolation method estimated the critical SCR as $SCR_{crit}^{conv} = 2.96$, while the proposed nonlinear method identified $SCR_{crit}^{prop} = 1.24$. The lower critical SCR obtained through the proposed approach aligns with the expected weak-grid instability characteristics of GFL converters. Figures 6– 7 show the PLL angle θ_{PLL} and frequency deviation $\Delta\omega_{PLL}$ responses at different grid strengths. For $SCR > 1.24$, the system exhibited well-damped behavior, whereas at $SCR = 1.24$, the PLL response diverged rapidly, leading to loss of synchronization. The phase portrait in Fig. 8 confirms this behavior, where the unstable trajectory moved far away from equilibrium, representing PLL-driven instability in weak-grid conditions, in accordance with the Lyapunov's stability theory.

These results verify that the proposed α-curve-based estimation captures the critical stability boundary more accurately without relying on linear approximations. It provides a continuous and physically interpretable stability margin across the entire SCR spectrum, revealing the converter's nonlinear response characteristics.

Table II summarizes the critical SCR values obtained from both the proposed α-curve method and the conventional linear extrapolation method. The extrapolation approach tends to either overestimate or underestimate the critical point, particularly when the α–SCR relationship is nonlinear.

TABLE II
COMPARISON OF CRITICAL SCR ESTIMATION METHODS

Converter Type	Conventional	Proposed Method
GFM (VSG-based)	9.47	11.95
GFL (PLL-based)	2.96	1.24

Overall, the proposed trajectory-sensitivity-based α-curve method successfully captures the contrasting stability trends of GFM and GFL converters. Unlike the conventional linear

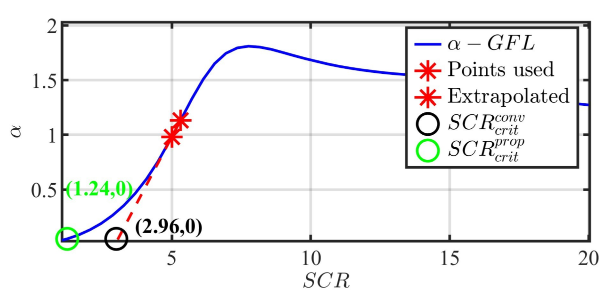

Fig. 5. Variation of the trajectory-sensitivity-based stability index α with SCR for PLL-based GFL.

979-8-3315-8138-1

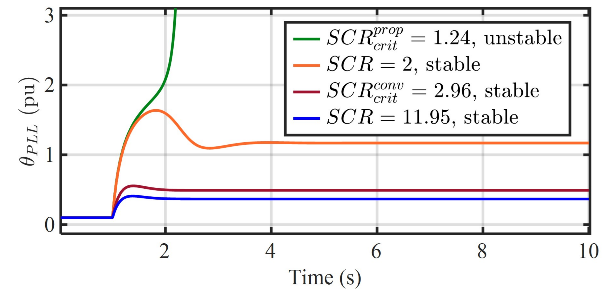

Fig. 6. PCC angle response of GFL under varying grid strengths.

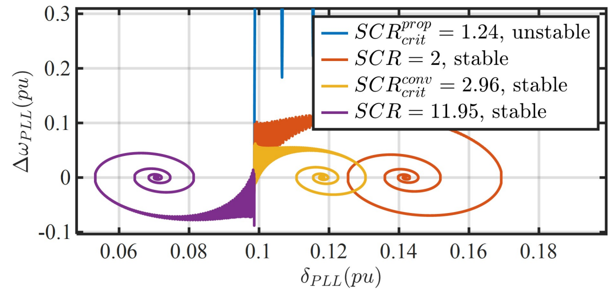

Fig. 8. Phase portraits illustrating stability transition in GFL.

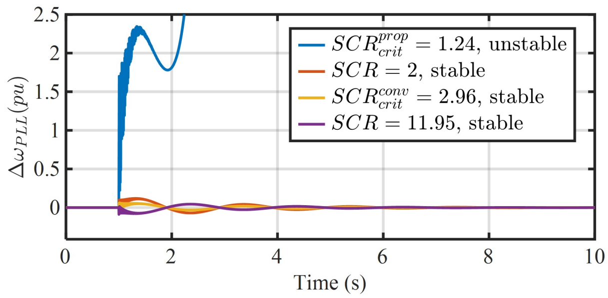

Fig. 7. Frequency deviation of GFL under varying grid strengths.

extrapolation approach, it inherently accounts for nonlinear converter–grid interactions, providing more accurate and physically meaningful critical SCR estimations.

V. Conclusion

This paper introduces a trajectory sensitivity-based method for evaluating the critical SCR of GFL and GFM inverters. By employing the $\mathcal{L}_2$-norm of sensitivity trajectories and a new stability index, α, the proposed framework identifies the instability threshold without reliance on linear approximations. It offers deeper insight into the evolution of sensitivity trajectories near the stability boundary, establishing a unified analytical framework for assessing converter stability as a function of grid strength. Future work will extend the proposed TSA-based framework to multi-parameter sensitivity analysis, including grid X/R ratio and validate against experimental hardware while also applying it to IEEE benchmark systems, where network topology, multiple converters, and interaction effects may further influence α-curve characteristics. Additionally, further theoretical investigation of α-curve behavior near the stability boundary will be pursued to enhance the robustness of critical parameter identification.

References

[1] B. Kroposki, B. Johnson, Y. Zhang, V. Gevorgian, P. Denholm, B.-M. Hodge, and B. Hannegan, "Achieving a 100 % renewable grid: Operating electric power systems with extremely high levels of variable renewable energy," *IEEE Power and Energy Magazine*, vol. 15, no. 2, pp. 61–73, 2017.

[2] W. Du, F. K. Tuffner, K. P. Schneider, R. H. Lasseter, J. Xie, Z. Chen, and B. Bhattarai, "Modeling of grid-forming and grid-following inverters for dynamic simulation of large-scale distribution systems," *IEEE Transactions on Power Delivery*, vol. 36, no. 4, pp. 2035–2045, 2021.

[3] H. Zhao *et al.*, "Small-signal stability analysis and control design of grid-connected inverter under weak grid conditions," *IEEE Transactions on Power Electronics*, vol. 34, no. 9, pp. 9259–9271, 2019.

[4] J. Z. Zhou, H. Ding, S. Fan, Y. Zhang, and A. M. Gole, "Impact of short-circuit ratio and phase-locked-loop parameters on the small-signal behavior of a vsc-hvdc converter," *IEEE Transactions on Power Delivery*, vol. 29, no. 5, pp. 2287–2296, 2014.

[5] M. Osman, N. Segal, A. Najafzadeh, and J. Harris, "Short-circuit modeling and system strength," *North American Electric Reliability Corporation, Atlanta, GA, White Paper*, 2018.

[6] Y. Li, Y. Gu, and T. C. Green, "Revisiting grid-forming and grid-following inverters: A duality theory," *IEEE Transactions on Power Systems*, vol. 37, no. 6, pp. 4541–4554, 2022.

[7] R. Yin, Y. Sun, S. Wang, and L. Zhang, "Stability analysis of the grid-tied vsc considering the influence of short circuit ratio and x/r," *IEEE Transactions on Circuits and Systems II: Express Briefs*, vol. 69, no. 1, pp. 129–133, 2022.

[8] K. De Brabandere, B. Bolsens, J. Van den Keybus, A. Woyte, J. Driesen, and R. Belmans, "A voltage and frequency droop control method for parallel inverters," *IEEE Transactions on Power Electronics*, vol. 22, no. 4, pp. 1107–1115, 2007.

[9] "IEEE Standard for Interconnection and Interoperability of Distributed Energy Resources with Associated Electric Power Systems Interfaces," 2018.

[10] A. Etxegarai, P. Eguia, E. Torres, A. Iturregi, and V. Valverde, "Review of grid connection requirements for generation assets in weak power grids," *Renewable and Sustainable Energy Reviews*, vol. 41, pp. 1501–1514, 2015.

[11] A. Pal and B. K. Panigrahi, "An enhanced inertial droop control for minimal sensitivity of grid-forming inverter interface to dynamic grid conditions," *IEEE Transactions on Power Delivery*, vol. 40, no. 4, pp. 1920–1933, 2025.

[12] X. Gao, D. Zhou, A. Anvari-Moghaddam, and F. Blaabjerg, "A comparative study of grid-following and grid-forming control schemes in power electronic-based power systems," *Power Electronics and Drives*, vol. 8, pp. 1–20, 01 2023.

[13] I. Hiskens and M. Pai, "Trajectory sensitivity analysis of hybrid systems," *IEEE Transactions on Circuits and Systems I: Fundamental Theory and Applications*, vol. 47, no. 2, pp. 204–220, 2000.

[14] U. Buragohain, A. S. Mir, and N. Senroy, "Transient stability assessment of a dfig-wtg system using trajectory sensitivity analysis," *IEEE Transactions on Power Systems*, vol. 39, no. 4, pp. 5818–5828, 2024.

[15] T. Nguyen, M. Pai, and I. Hiskens, "Sensitivity approaches for direct computation of critical parameters in a power system," *International Journal of Electrical Power & Energy Systems*, vol. 24, no. 5, pp. 337–343, 2002.

[16] S. D'Arco, J. A. Suul, and O. B. Fosso, "A virtual synchronous machine implementation for distributed control of power converters in smartgrids," *Electric Power Systems Research*, vol. 122, pp. 180–197, 2015.

[17] J. Suul, S. D'Arco, P. Rodriguez, and M. Molinas, "Impedance-compensated grid synchronisation for extending the stability range of weak grids with voltage source converters," *IET Generation, Transmission Distribution*, vol. 10, 01 2016.